Tailoring the electronic structure of TiO_2 by cation codoping from hybrid density functional theory calculations

Run Long* and Niall J. English†

The SEC Strategic Research Cluster and the Centre for Synthesis and Chemical Biology, School of Chemical and Bioprocess Engineering, University College Dublin, Belfield, Dublin 4, Ireland

(Received 13 January 2011; revised manuscript received 7 February 2011; published 20 April 2011)

The large intrinsic band gap in TiO_2 has hindered severely its potential application for visible-light irradiation, while anion doping has led to decreases in visible-light photocatalytic activity in spite of narrowing the host band gap. In this study, we have used cation-passivated codoping of Mo with Zn/Cd and also of Ta with Ga/In to modify the band edges of anatase-TiO_2 to extend absorption to longer visible-light wavelengths using the generalized Kohn-Sham theory with the Heyd-Scuseria-Ernzerhof (HSE06) hybrid functional for exchange and correlation. It has been found that (Mo,Zn/Cd)-codoped systems can narrow the band gap significantly and passivate gap states. Considering the host and impurity ionic radii, it is expected that Mo with Zn should constitute the best cationic dopant pair.

DOI: 10.1103/PhysRevB.83.155209 PACS number(s): 71.20.Nr

I. INTRODUCTION

Titanium dioxide (TiO_2) is an effective photocatalyst for the decomposition of organic pollutants and is a promising candidate material for possible applications in solar energy conversion.[1] However, its universal use is restricted to ultraviolet light ($\lambda < 385$ nm) due to the wide band gap of titania ($\sim$3.2 eV for anatase). Further, photoexcited electron-hole pairs tend to recombine relatively easily in TiO_2. Both of these factors limit possible applications in photocatalytic materials design. Therefore, tailoring the band gap of TiO_2 to make it photosensitive to visible light with low electron-hole recombination is one of the most important objectives in photocatalyst studies.

In general, doping is one of the most effective approaches to extend the absorption edge to the visible-light range, involving either the introduction of isolated impurity states into the forbidden gap or narrowing the band gap. For instance, doping with transition-metal cations (e.g., Cr, V, W) at Ti sites and anions (e.g., N, C, S) at O sites are the two main methods currently in use.[2–6] Since O 2*p* orbitals dominate the valence band (VB) and Ti 3*d* orbitals govern the conduction band (CB), anion doping serves mostly to modify the VB of TiO_2 due to different *p* orbitals *vis-à-vis* O 2*p* states, while cation doping usually produces gap states in the forbidden gap or resonates with the bottom of the CB.[4] However, the extent of band-gap narrowing is limited with monodoping. Recent theoretical works have indicated that codoping of anions with cations not only narrows the band gap significantly, but also serves to largely counteract the presence of recombination centers.[7,8] It should be noted, however, that anion-doped TiO_2 usually shows a lower photocatalytic activity under visible light than UV light because the oxidative power and mobility of photogenerated holes in the isolated states are lower than those in the VB of TiO_2.[5] However, if either isolated states can be created below the CB or the host band gap narrowed by codoping with two kinds of cations while allowing TiO_2 to absorb visible light, this would be expected to overcome this shortcoming, at least in part. On the other hand, isolated states could serve as carrier recombination centers,[9] which will reduce photocatalytic efficiency. At the same time, even if the isolated states are fully occupied, band-to-band transitions are much more effective than localized state-to-band transitions, due to a much larger intensity. On the conceptual basis of narrowing band gaps without creating isolated states and movements of the VB,[7,10] we have attempted to design novel and efficient visible-light-activated TiO_2-based photocatalysts via cation codoping.

The two essential criteria for the selection of cations for codoping are as follows: (i) similar Ti^{4+} (d^0) electronic configurations, with the cations having similar closed-shell electronic configurations, d^0 or d^{10}; (ii) codoping with cations A^{x+} and B^{y+} should retain the semiconductor characteristics of TiO_2, namely $x + y = 8$. As a consequence, four pairs of cations were chosen from the set (Mo^{6+},Zn^{2+}/Cd^{2+}) and (Ta^{5+},Ga^{3+}/In^{3+}), in which the cations *A* (Mo^{6+},Ta^{5+}) have d^0 electronic configurations while cations *B* (Zn^{2+},Cd^{2+},Ga^{3+},In^{3+}) possess d^{10} configurations.

II. METHODOLOGY

We apply the spin-polarized density functional theory (DFT) calculations using the projector augmented wave (PAW) pseudopotentials as implemented in the Vienna *ab initio* Simulation Package (VASP) code.[11,12] The calculations were performed using the hybrid functional Heyd-Scuseria-Ernzerhof (HSE06) hybrid functional.[13–15] The exchange potential employed in the HSE06 is divided into short- and long-range parts, and Hartree-Fock (HF) exchange is mixed with Perdew-Burke-Ernzerhof (PBE)[16–18] exchange in the short-range part. To avoid the expensive calculation of long-range HF exchange, this term is replaced by long-range PBE exchange. The electron wave function was expanded in plane waves up to a cutoff energy of 400 eV, and a Monkhorst-Pack *k*-point mesh[19] of $2 \times 2 \times 2$ was used for geometry optimization and electronic-structure calculations. Both the atomic positions and cell parameters were optimized until residual forces were below 0.01 eV/Å. We used a 108-atom supercell containing 72 O atoms and 36 Ti atoms to simulate bulk anatase TiO_2, arising from $3 \times 3 \times 1$ replication of the anatase unit cell, as shown in Fig. 1.

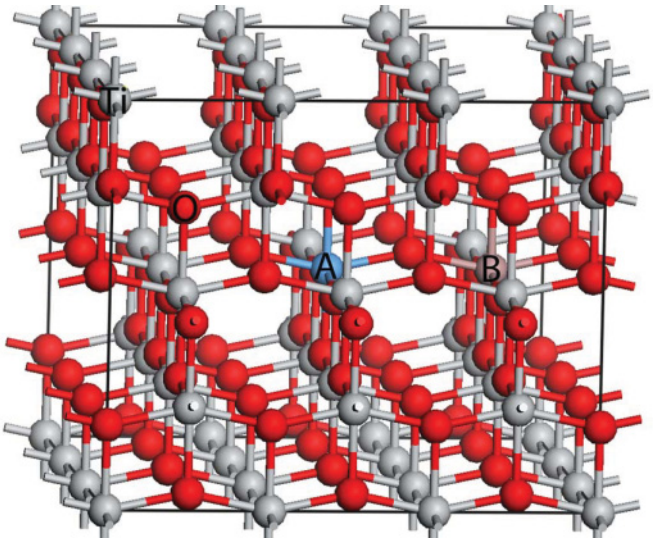

FIG. 1. (Color online) Supercell model for cation pair $A(d^{10})$-$B(d^0)$-codoped anatase showing the location of the dopants. The ion doping sites are marked by A and B.

III. RESULTS AND DISCUSSION

A. Monodoping in anatase

In this section, our main concern is to investigate how to engineer the band edges of TiO_2 using a single cation dopant. Before investigation of the influence of dopants on the electronic structure of TiO_2, the density of states (DOS) and projected DOS (PDOS) of pure anatase are plotted in Fig. 2. Clearly, the O 2p states dominate the valence-band edge, and Ti 3d states govern the conduction-band edge, respectively, leading to a band gap of 3.55 eV, close to an experimental value of 3.2 eV.[20] It is to be hoped that cation monodoping could either change the position of the CB edge or produce impurity states below the CB.

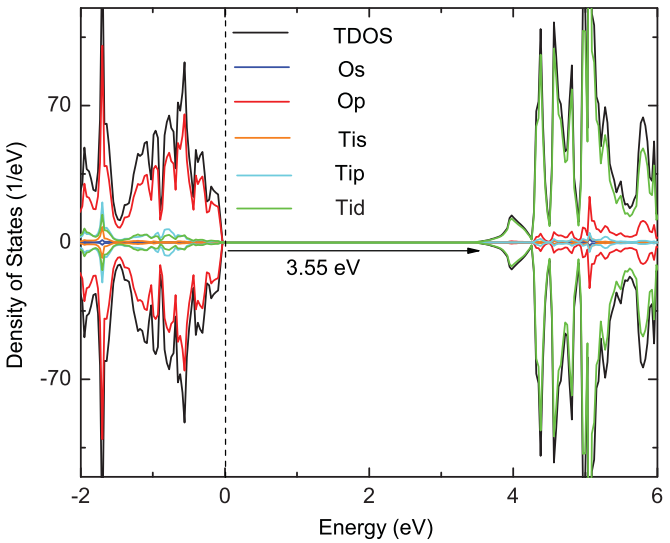

FIG. 2. (Color online) The HSE06-calculated total and projected density of states (PDOS) of anatase TiO_2. The highest occupied state is chosen as the Fermi energy and is set to zero.

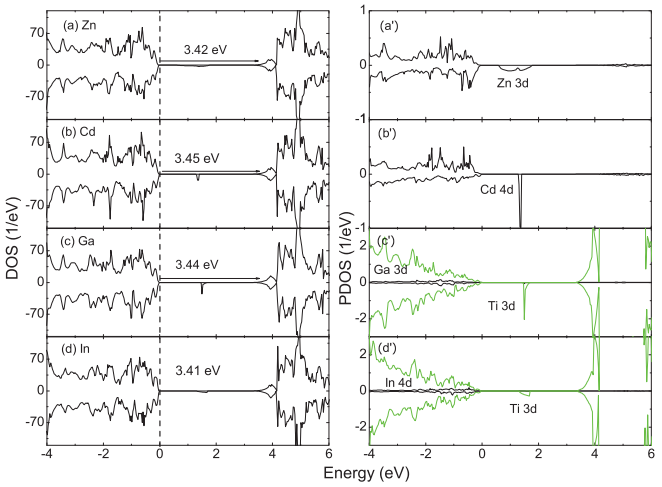

FIG. 3. (Color online) Density of states (DOS) and PDOS for Zn, Cd, Ga, and In (d^{10} electron configuration)-monodoped anatase. The top of the valence band of pure 108-atom anatase is set as zero.

First, the DOS and PDOS of Zn, Cd, Ga, and In (d^{10} electron configuration)-doped TiO_2 systems are shown in Fig. 3. In the replacement of Ti atoms by such metal elements, the 3d orbitals of Zn and 4d orbitals of Cd not only contribute to the top of the VB, but also to the states in the forbidden gap. Here, the dopants result in a slight gap narrowing, and the gap states are also beneficial for electron transition. Both of them may serve to extend absorption to the visible-light region, which can explain the results reported by experiments that Zn/Cd-doped TiO_2 possesses high visible-light activity.[21,22] On the other hand, the 3d orbitals of Ga and 4d states of In only contribute to the top of the valence band, and some of these reside well within the conduction band, and there is a slight contribution to gap narrowing.[23,24] However, both of the dopants bring local lattice distortion and form an "oxygen-vacancy-like" defect, which reduces the second-neighboring Ti^{4+} into "Ti^{3+}" ion that produce Ti^{3+} gap states in the forbidden gap responsible for harvesting longer visible light reported by experiments.[23,24] Therefore, d^{10} metals including Zn, Cd, Ga, and In will either contribute to the top of the valence band or produce impurity states in the forbidden gap. As shown here, although each of the narrowings in the band gap is quite small, the gap state-to-band transition should be responsible for high photocatalytic activity reported in experiments under visible-light irradiation.[21–24] Secondly, the calculated DOS and PODS of Mo and Ta (d^0 electron configuration)-doped TiO_2 systems are shown in Fig. 4. For Ta-doped TiO_2 [cf. Fig. 4(a)], the band gap is slightly reduced by 0.07 eV relative to pure anatase (3.55 eV). However, the Ta^{5+} ion is reduced via Ti^{4+} into the "Ti^{3+}" ion, and the "Ti^{3+}" gap state is located below the CB, which can offer a bridge for electron transition to extend optical absorption to the visible-light region, while the band gap of Mo-doped TiO_2 [cf. Fig. 4(b)] is slightly reduced by 0.09 eV *vis-à-vis* pure TiO_2. Here, the localized states below the CB arise mainly from both Mo^{6+} and slightly from "Ti^{3+}" ions, which is different from Ta-doped TiO_2, but this is beneficial for electron transition as well. However, the magnetic moment of 2.0 μB per supercell indicates that the Mo ion is in the Mo^{6+} oxidation state in Mo-doped TiO_2, which is similar to

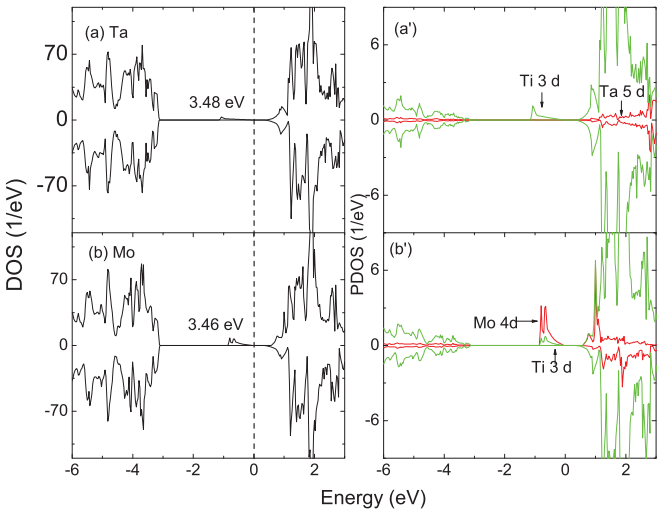

FIG. 4. (Color online) DOS and PDOS for Ta and Mo (d^0 electron configuration)-monodoped 108-atom anatase. The top of the valence band of pure anatase is set as zero.

1.0 μB per supercell of Ta^{5+} in Ta-doped TiO_2. To check our calculations, the DOS and PDOS of a Mo-doped 48-atom supercell were also plotted in Fig. 5, and they also indicate that Mo dominates the gap states. The magnetic moment is the same as that of the Mo-doped TiO_2 supercell. Previous experimental studies show that TiO_2 doped with Mo^{6+} and Ta^{5+} possesses substantially higher photocatalytic activity than that of pure TiO_2 due to the effective separation of charge carriers.[25,26] Therefore, intermediate electronic bands below the CB originating from dopants and "Ti^{3+}," which could harvest a longer optical absorption edge, are expected. The gap narrowing is still small here, as well as the top of the VB moving to lower energy, so that photocatalytic activity should be reduced according to the previous experiment.[5] Although monodoping of d^0 and d^{10} electron dopants produces localized states in the forbidden gap for improvement of visible-light activity, localized state-to-band transitions are under band-to-band transitions due to a much smaller intensity. It is expected that n-p-compensated codoped d^0-d^{10} cation pairs will lead to larger band-gap reductions without gap states and movement of the VB.

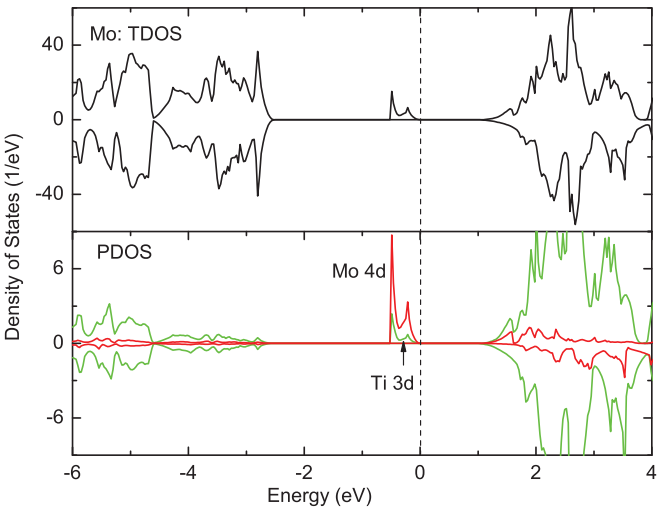

FIG. 5. (Color online) DOS and PDOS for Ta and Mo (d^0 electron configuration)-monodoped 48-atom anatase. The top of the valence band of pure anatase is set as zero.

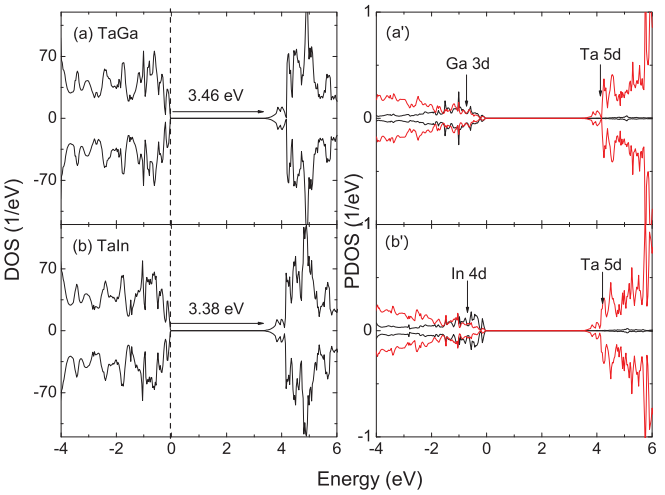

FIG. 6. (Color online) DOS and PDOS for (Ta,Ga/In)-codoped 108-atom supercell anatase. The top of the valence band of pure anatase is set as zero.

B. Codoping in anatase

Codoping of d^{10}-based (Zn, Cd, Ga, and In) with d^0-configuration (Mo and Ta) metal dopants may serve to narrow the band gap and maintain charge neutrality simultaneously. It is also to be expected that codoping should not lead to a decrease in the photocatalytic activity without a change in the position of the VB. The DOS and PDOS of Ta and Ga/In-codoped anatase are shown in Fig. 6, while those for the Mo and Zn/Cd cases are plotted in Fig. 7. As shown in Fig. 6, although the gap states were passivated by codoping, the band gap is reduced slightly in both (Ta,Ga)- and (Ta, In)-codoped TiO_2. Compared to Ga-, In-, and Ta-monodoped TiO_2, codoping cannot extend obviously the absorption edge

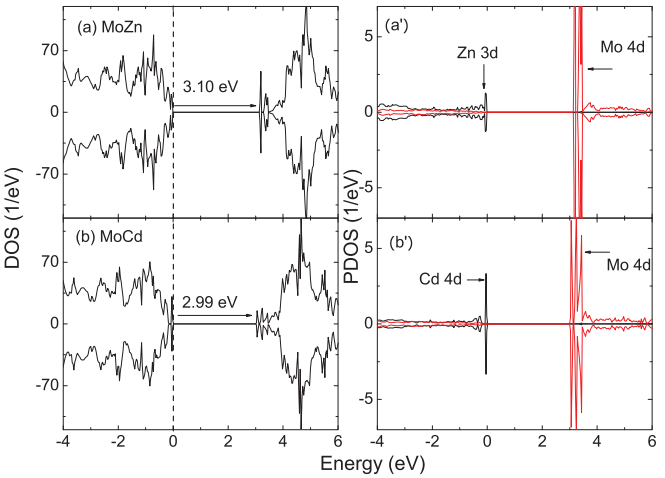

FIG. 7. (Color online) DOS and PDOS for (Mo^{6+},Zn/Cd)-codoped 108-atom anatase. The top of the valence band of pure anatase is set as zero.

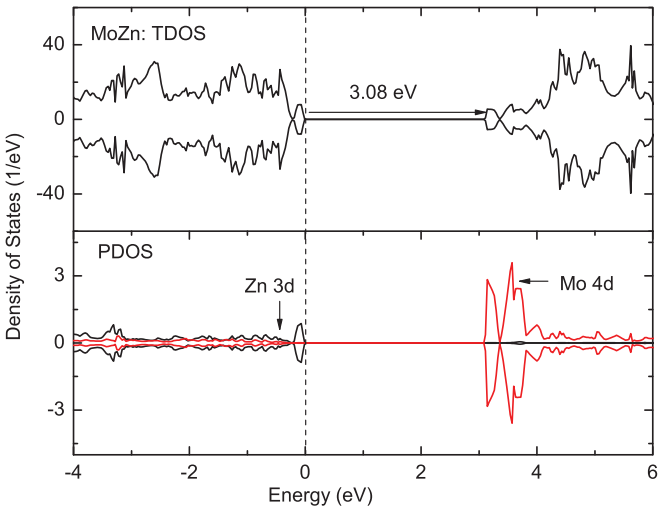

FIG. 8. (Color online) Total density of states (TDOS) and PDOS for (Mo,Zn)-codoped 48-atom anatase TiO_2. The top of the valence band of pure anatase is set as zero.

to the longer-wavelength visible-light region. Fortunately, the gap narrowing is as large as 0.5 eV for (Mo,Zn)- and (Mo,Cd)-codoped TiO_2 (cf. Fig. 7) relative to the pure case, and both of them will harvest much more visible light relative to the monodoping cases. Zn 3*d* and Cd 4*d* are situated at the top of the VB, and the 4*d* states of Mo dominate the bottom of the CB, which tends to lead to high-efficiency band-to-band transitions *vis-à-vis* their respective monodoped configurations. Furthermore, here, band-gap narrowing is derived from the movement of the bottom of the CB to lower energies rather than movement of the top of the VB; these satisfy well the requirements of narrowing the band gap without decreasing the photocatalytic activity.[5] Moreover, localized states are canceled due to *n-p* compensated codoping in all of the studied systems. Therefore, Mo- and Zn/Cd-codoped TiO_2 can effectively reduce the host band gap significantly, as well as a downshift of CB and passivation of gap states, which is likely to increase visible-light photocatalytic activity. The matching of ionic radii to each other is another factor to be considered experimentally. Here, the effective ionic radius of Mo^{6+} is 0.59 Å, while for Zn^{2+} (four-coordinate) and Cd^{2+} (four-coordinate), the respective radii are 0.64 and 0.78 Å. Therefore, since the ionic radii of Mo^{6+} and Zn^{2+} are similar to that of Ti^{4+} (0.61 Å),[26] this would suggest that Mo^{6+}-Zn^{2+} should act as the best cation pair due to their similar ionic radii.

To check the influence of doping concentration on electronic structure, we have also performed HSE06 calculations for the 48-atom supercell with (Mo,Zn)-codoped TiO_2. The calculated DOS and PDOS are similar to the behavior of a 108-atom supercell, as displayed in Fig. 8. The obtained band gap for the (Mo,Zn)-codoped 108-atom supercell TiO_2 is 3.08 eV, a little smaller than the value predicted from the 108-atom supercell (3.11) eV, indicating that the increasing doping concentration is beneficial for gap narrowing.

IV. CONCLUSIONS

Based on HSE06 functional calculations and analysis of electronic structures, we propose that (Mo + Zn)-codoped TiO_2 is a strong candidate for visible-light photocatalysts without decreasing the photocatalytic activity, because it reduces the band gap largely by inducing a downshift in the bottom of the conduction band, passivating the impurity states as well their similar ionic radii *vis-à-vis* each other and Ti^{4+}. This method can be applied to tailor the band structure of other wide-bad-gap semiconductors, such as ZnO, In_2O_3 and so on.

ACKNOWLEDGMENTS

This work was supported by the IRCSET-Marie Curie International Mobility Fellowship in Science, Engineering and Technology. The authors thank Science Foundation Ireland and the Irish Centre for High End Computing for the provision of computational resources.

*run.long@ucd.ie
†niall.english@ucd.ie

[1] M. R. Hoffmann, S. T. Martin, W. W. Choi, and D. W. Bahnemann, Chem. Rev. **95**, 69 (1995).
[2] E. Borgarello, J. Kiwi, M. Grätzel, E. Pelizzetti, and M. Visca, J. Am. Chem. Soc. **104**, 2996 (1982).
[3] K. S. Yang, Y. Dai, and B. B. Huang, J. Phys. Chem. C **111**, 18985 (2007).
[4] R. Asahi, T. Morikawa, T. Ohwaki, K. Aoki, and Y. Taga, Science **293**, 269 (2001).
[5] H. Irie, Y. Watanabe, and K. Hashimoto, J. Phys. Chem. B **107**, 5483 (2003).
[6] T. Umebayashi, Y. Yamaki, H. Itoh, and K. Asai, Appl. Phys. Lett. **81**, 454 (2002).
[7] Y. Q. Gai, J. B. Li, A. S. Li, J. B. Xia, and S. H. Wei, Phys. Rev. Lett. **102**, 036402 (2009).
[8] R. Long and N. J. English, Appl. Phys. Lett. **94**, 132102 (2009).
[9] K. S. Ahn, Y. F. Yan, S. Shet, T. Deutsch, J. Turner, and M. Al-Jassim, Appl. Phys. Lett. **91**, 231909 (2007).
[10] H. G. Yu, H. Irie, and K. Hashimoto, J. Am. Chem. Soc. **132**, 6898 (2010).
[11] G. Kresse and J. Hafner, Phys. Rev. B **47**, 558 (1993).
[12] G. Kresse and J. Furthmüller, Phys. Rev. B **54**, 11169 (1996).
[13] J. Heyd, G. E. Scuseria, and M. Ernzerhof, J. Chem. Phys. **118**, 8207 (2003).
[14] J. Paier, M. Marsman, K. Hummer, G. Kress, I. C. Gerber, and J. G. Angyan, J. Chem. Phys. **125**, 249901 (2006).
[15] J. Heyd, G. E. Scuseria, and M. Ernzerhof, J. Chem. Phys. **124**, 219906 (2006).
[16] A. D. Becke, J. Chem. Phys. **98**, 1372 (1993); **99**, 5648 (1993).
[17] J. P. Perdew, K. Burke, and M. Ernzerhof, Phys. Rev. Lett. **77**, 3865 (1996).
[18] H. J. Monkhorst and J. D. Pack, Phys. Rev. B **13**, 5188 (1976).

[19]H. Tang, H. Berger, P. E. Schmid, and F. Lévy, Solid State Commun. **87**, 847 (1993).
[20]Y. Zhao, C. Z. Li, X. H. Liu, F. Gu, H. L. Du, and L. Y. Shi, Appl. Catal., B **79**, 208 (2008).
[21]L. Andronic, A. Enesca, C. Vladuta, and A. Duta, Chem. Eng. J. **152**, 64 (2009).
[22]J. K. Zhou, Y. X. Zhang, X. S. Zhao, and A. K. Ray, Ind. Eng. Chem. Res. **45**, 3503 (2006).
[23]E. J. Wang, W. S. Yang, and Y. A. Cao, J. Phys. Chem. C **113**, 20912 (2009).
[24]C. H. Wang, A. F. Geng, Y. H. Guo, S. J. Jiang, and X. S. Qu, Mater. Lett. **60**, 2711 (2006).
[25]G. Devi and B. N. Murthy, Catal. Lett. **125**, 320 (2008).
[26]*CRC Handbook of Chemistry and Physics*, 87th ed., edited by D. R. Lide (Taylor & Francis, London, 2006).